

# Interconnection of Norway to European Balancing Platforms Using Hierarchical Balancing

1<sup>st</sup> Anthony Papavasiliou

Department of Electrical and Computer Engineering  
National Technical University of Athens  
Athens, Greece  
papavasiliou@mail.ntua.gr

2<sup>nd</sup> Gerard Doorman

Statnett SF  
Oslo, Norway  
Gerard.Doorman@statnett.no

3<sup>rd</sup> Mette Bjørndal

Business and Management Science  
Norwegian School of Economics  
Bergen, Norway  
mette.bjorndal@nhh.no

4<sup>th</sup> Yves Langer

N-SIDE  
Louvain la Neuve, Belgium  
yla@n-side.com

5<sup>th</sup> Guillaume Leclercq

N-SIDE  
Louvain la Neuve, Belgium  
gle@n-side.com

6<sup>th</sup> Pierre Crucifix

N-SIDE  
Louvain la Neuve, Belgium  
pcu@n-side.com

**Abstract**—In order to cope with intra-zonal grid constraints, we propose a hierarchical paradigm for organizing balancing and congestion management in European zonal markets. Our approach relies on an aggregation function which converts balancing market offers to zonal market offers that adhere to the bidding format of European balancing platforms, followed by a disaggregation function for dispatching and settlement which represents physical constraints of network flow. We investigate various design choices related to our proposed aggregation-disaggregation paradigm. We test our proposed methodology on a 46-node model of the Nordic system by reporting on a variety of technical and economic performance metrics.

**Index Terms**—Balancing, congestion management, nodal pricing, zonal pricing, Benders decomposition.

## I. INTRODUCTION

### A. Context

Following the integration of European day-ahead and intraday electricity markets, European balancing operations are following suit with the rollout of pan-European balancing platforms. A weakness of the platforms that are being rolled out is the zonal representation of the underlying network. This zonal representation is inherited from the day-ahead and intraday European market design.

Zonal market clearing can threaten system security [5]. Since the physical laws of power flow are not represented accurately, zonal dispatch may lead to network overloads. Whereas there is time to correct such overloads in day-ahead or intraday operations, balancing operation time-frames can be unforgiving since there is almost no time left to system operators for re-dispatching units in order to correct network overloads.

In anticipation of this challenge, Norwegian TSO Statnett is presently implementing a “bid filtering” approach, which attempts to identify bids that may cause overloads if activated, and make them unavailable for the balancing platforms [3]. However, the approach is still under development and has

several drawbacks, and Statnett is therefore also investigating alternative solutions. One such solution is *hierarchical balancing*. This approach was originally proposed by the authors in [7], where it was illustrated in a classical instance from the literature, the six-node two-zone system of Chao and Peck [8]. The approach has also been proposed and tested in the context of transmission-distribution coordination [6].

### B. Paper Contribution and Organization

The present paper investigates a number of detailed design options of the hierarchical balancing proposal by testing them on a 46-node model of the Nordic system. The case study focuses on the integration of Norway to the MARI platform<sup>2</sup> (MARI, which stands for “Manually Activated Reserves Initiative”, is the pan-European platform for the activation of manual frequency restoration reserve, abbreviated hereafter as mFRR [1]). The specific options that we investigate in our work are the resolution of the residual supply functions (that represent the commercial bids in the MARI platform), whether or not we assume coordinated balancing in the aggregation stage of the hierarchical coordination, and whether or not we apply nodal prices at the pricing stage of the disaggregation. We propose and report a number of metrics for assessing the technical and economic performance of alternative proposals.

The paper is organized as follows. In section II we describe the hierarchical balancing paradigm. In section III we describe the different design options and the associated tradeoffs. In section IV we present our case study and report and comment on our findings. Section V concludes.

## II. HIERARCHICAL BALANCING

### A. Description of the Process

Fig. 1 presents the sequence of events in hierarchical balancing. We describe the steps of the process in the sequel.

<sup>2</sup>Note that the concept of hierarchical balancing is more general than MARI, and can apply to a general Activation Optimization Function (AOF) for balancing.

The notation which is used and the associated models are summarized in the appendix.

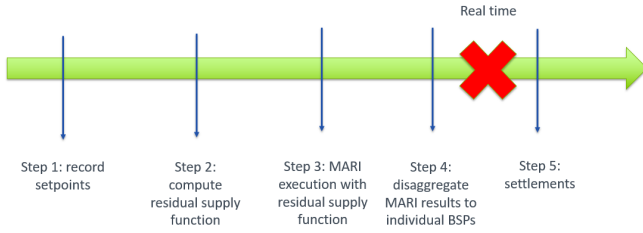


Fig. 1: Timeline of hierarchical balancing.

**Step 1: record setpoints.** This step of the process requires the Norwegian TSO<sup>3</sup> to collect measurements and calculate (i) baseline flows  $F_k^{Base}$ ,  $k \in K_{NO}$ , in the Norwegian system, and (ii) the set-points  $P_g^0$ ,  $g \in G_B$ , of Norwegian balancing resources.

**Step 2: compute residual supply function.** We assume that this step, as well as step 4, are performed by an *Aggregation-Disaggregation System (ADS)*, as indicated in Fig. 1. This is a service that is executed on behalf of the Norwegian TSO. Step 2 of the process collects Norwegian balancing offers, and uses them as the basis to construct synthetic bids that reflect actual bids submitted by balancing service providers (BSPs) while also accounting for any intra-zonal constraints. This is motivated by the fact that MARI does not recognize such internal constraints, which nevertheless would result in unacceptable security violations if specific bids would be activated. Our proposed hierarchical balancing approach aims at handling this misalignment between physics and the zonal model as gracefully as possible by constructing one *residual supply function* (abbreviated RSF hereafter) per Norwegian zone. The RSFs map the total amount of balancing energy produced in a given Norwegian zone to the incremental cost of producing said energy. The aggregation model is presented in the appendix.

**Step 3: MARI execution.** In this step the MARI platform clears with BSP offers from non-Norwegian zones and the Norwegian RSFs. What the Norwegian TSO receives as output from this step are the zonal prices from the MARI platform, as well as a net balancing position for each Norwegian zone. The MARI clearing model is presented in the appendix.

**Step 4: disaggregate MARI results to individual BSPs.** This step of the process consists of two separate computations, a quantity disaggregation step (step 4a) and a price disaggregation step (step 4b). In the quantity disaggregation step, the Norwegian TSO computes dispatch setpoints for Norwegian BSPs, given the total zonal export target of each Norwegian zone, as determined by MARI. In the price disaggregation step, the TSO computes nodal settlement prices for the Norwegian buses which aim at producing incentives that are coherent with the profit maximization objective of individual BSPs and the use of the network given the decisions that are determined

<sup>3</sup>In the following “the Norwegian TSO” is used in a generic way. The description is based on an ongoing research project, and the results are far from being implemented in real life.

at the quantity disaggregation step, while also attempting to remain as close as possible to the MARI zonal prices. Both the quantity and the price disaggregation steps are described mathematically in the appendix.

**Step 5: settlements.** This step is performed after real-time operations. It determines cash flows between market agents, and is illustrated in detail in the results section.

### B. Illustration on a Single Imbalance Realization

In order to run MARI, we require a realization of imbalances at a zonal level. Consider the imbalances reported in Table I (see section IV-C for a description of how imbalance samples are generated). The table also indicates the net position of each Norwegian zone, as well as the solution produced by an optimal power flow (OPF). Note that, when referring to “net position” in the caption of Table I, we mean  $E_z = \sum_{n=1}^{N_{RSF}} p_{zn}$ , i.e. the output of each aggregate Norwegian BSP in each zone.

TABLE I: Imbalances (row 2) and zonal net positions under the baseline approach (row 3) and the OPF solution (row 4).

	NO1	NO2	NO3	NO4	NO5	Total
Imb. (MW)	-328.3	-141.2	-42.6	-208.4	-199.9	-920.3
Base (MW)	101.8	99.8	49.8	154.1	75.7	481.3
OPF	240.0	240.0	0.0	120.0	240.0	840.0

The MARI prices for Norway are presented in Fig. 2. Congested links are indicated in red font, and the congestion is from North to South.

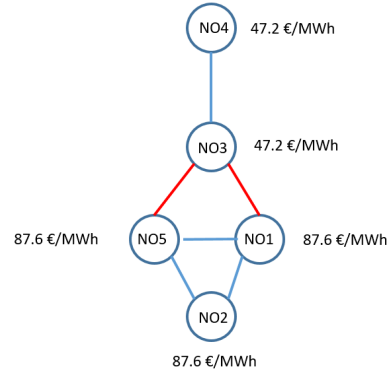


Fig. 2: MARI clearing prices for Norwegian zones in step 3. Red interconnections indicate congestion.

The results of the price disaggregation for this specific imbalance realization are reported in Table II. We observe that the prices are identical for all nodes of each zone, which is consistent with the fact that there is no congestion within zones for this specific instance in the quantity disaggregation of step 4.

Fig. 2 indicates price separation in the MARI market clearing solution. The aggregation of the hierarchical approach accounts for the overloading of a particular line within NO1, when building the RSF. MARI does not account for this line individually when activating the NO1 RSF, and the RSF is constructed assuming that no imbalances occur and that the net position of all other zones is zero.

TABLE II: Minimum local BSP price and maximum local BSP price generated in step 4b, compared to the MARI zonal price of step 3. All quantities are in €/MWh.

	NO1	NO2	NO3	NO4	NO5
Min. price	35.40	31.35	47.25	45.73	34.86
Max. price	35.40	31.35	47.25	45.73	34.86
MARI price	87.64	87.64	47.25	47.25	87.64

We close the simulation chain by reporting the settlements that take place in the different steps of the procedure. The settlements are presented in Table III, and are based on the prices reported in Table II. The table has been designed such that every row sums to zero, meaning that each row corresponds to a precise cash flow from one or multiple agents to one or multiple agents. The columns correspond to agents that are involved in cash flows. The initials BRP refer to *balance responsible parties*, which correspond in our model to price-taking real-time energy imbalances. The fifth column corresponds to the cash flows of the ADS. We report the cash flows associated to this service separately, in order to keep the exposition more clear, but ADS cash flows can be thought of as a cash flow that affect “TSO Norway”, i.e. the second column.

### III. DESIGN OPTIONS

We now proceed to discuss certain design options and the associated tradeoffs.

#### A. Resolution of Residual Supply Functions

We analyze the sensitivity of the model to the granularity of the RSF. We are specifically interested in understanding the sensitivity of the dispatch to an increased resolution of the supply function.

The number of optimal power flows that need to be computed in order to generate the different RSFs is equal to the number of breakpoints times the number of zones. There are five zones in the Norwegian system. We perform tests ranging from 11 to 10001 breakpoints. The range of the RSF of each zone is determined by the maximum capacity of lines that interconnect each Norwegian zone to its neighboring zones. Given the range of each zone, the increments of the residual supply function for these different levels of resolution are then determined by the number of breakpoints. An alternative which is not tested in the present paper is to consider a constant MW increment in the discrete approximation of the RSFs.

Note that the minimum acceptable bid size in MARI is 1 MW. In Table IV we present the evolution of the net position of each Norwegian zone as a function of the number of breakpoints, and compare them with the optimal solution produced with the OPF solution for the entire system. The solution stabilizes beyond one thousand breakpoints. In the second row of the table, we report the corresponding value of the OPF solution. It is worth noting the difference between OPF and the “best-possible” version of the RSF (with 10001 breakpoints). We can conclude from this difference that there is no guarantee that the OPF solution can be reproduced by the RSF approach, since the RSF approach can only control what

happens within Norway, not outside. Naturally, the resulting dispatch will therefore almost always be more costly than an OPF.

Given the stable behavior of the RSFs beyond 1001 breakpoints observed in Table IV, we proceed for the remainder of the paper with a resolution of 1001 breakpoints.

#### B. Tight Versus Loose Aggregation

An important assumption in Eq. (5) is that, during the aggregation step that is required for building the residual supply function, zone  $z$  can benefit from resources in other Norwegian zones. An alternative assumption is to ignore the potential contribution of Norwegian resources other than zone  $z$  when computing the RSF  $TC_z(e)$  of that zone. We refer to this as *aggregation with loose coordination*, in order to contrast it to an aggregation with a tight coordination of Norwegian resources which is the assumption in the model of Eqs. (4) - (12). Concretely, we propose an alternative to the model of Eqs. (4) - (12), where equation (5) is replaced by

$$P_g^- \leq p_g + P_g^0 \leq P_g^+, g \in G_B : Z_g = z. \quad (1)$$

In this model, the Norwegian balancing production of all other zones than zone  $z$  is set to zero:

$$p_g = 0, g \in G_B : Z_g \in Z_{NO} - \{z\}. \quad (2)$$

This design choice can have a significant impact on the RSFs. We present the different RSFs for tight versus loose coordination in our case study in Fig. 3. The general effect of loose coordination is that it is more conservative in estimating what the zone can deliver as output, since it relies only on the individual resources of a given zone, without allowing other zones to reshuffle their dispatch in a balanced way. Note that tight coordination is more aligned with the integrated way in which we disaggregate dispatch in step 4a, where we assume that Norwegian zones can coordinate when delivering their target MARI export.

#### C. Aggregation with Clairvoyance

An important assumption that is adopted in the baseline model is that we do not account for imbalances when we execute the aggregation in step 2, i.e. we compute RSFs corresponding to a system that has not been confronted with the imbalance of the upcoming interval. Instead, one may assume that imbalances can be forecast with acceptable accuracy and in sufficient time to still allow the computation of the RSFs in step 2 before bidding into MARI. This motivates a new version of the hierarchical approach, which we refer to as *aggregation with clairvoyance*. The essential difference to the baseline approach is that constraint (8) of the RSF aggregation step is replaced by the following:

$$f_k = F_k^{Base} + \sum_{n \in N_{NO}} PTDF_{kn} \cdot (r_n + Imb_n), k \in K_{NO} - K_{DC} \quad (3)$$

This approach results in a different RSF per imbalance realization, whereas the baseline approach computes a unique RSF for every imbalance realization.

TABLE III: Settlement table for step 5. All reported values are in €.

	TSO Norway	BSPs Norway	BRPs Norway	ADS	MARI platform
MARI ADS and TSO demands	-70519	0	0	33940	36579
MARI within-Norway congestion rent	2019	0	0	0	-2019
MARI Norwegian border congestion rent	6906	0	0	0	-6906
Norway BSP disaggregation	0	18773	0	-18773	0
Norway BRP disaggregation	34555	0	-34555	0	0
Total	-27039	18773	-34555	15167	27654

TABLE IV: Net position (in MW) for each of the Norwegian zones as a function of the number of breakpoints.

	NO1	NO2	NO3	NO4	NO5
OPF	240	240	0	120	240
11	192	85.3	59.9	144	0
101	115.2	96	50.3	153.6	66.1
1001	101.8	99.8	49.8	154.1	75.7
10001	101.2	100.4	49.6	154.3	75.7

## IV. CASE STUDY

### A. The Nordic 46-Node System

We apply our analysis on a 46-node model of the Nordic system. The model originates from the Siemens PSSE model of Vanfretti [9], supplemented by data from the master thesis of Bøe [2]. Whereas the PSSE model of Vanfretti and the MSc thesis of Bøe are limited to technical data, we rely on expert input from Statnett in order to further populate the model with economic data related to the marginal cost profiles of balancing resources in the Nordics. The zonal network data of the model is further validated against NordPool data. We have further modified the original dataset in order to better align it to its current status by removing and adding a limited number of lines, adding an additional node to the model, and modifying a limited number of susceptance values. The final model that is used in our case study thus consists of 80 lines (AC lines, DC lines, and transformers), 46 nodes, and the Nordic zones (5 Norwegian zones, 4 Swedish zones and a single Finnish zone). The full dataset which is used in the study is uploaded online by the authors at the following link: <http://users.ntua.gr/papavasiliou/DatasetEEM2022.zip>. It should be noted that the model has only weak relations to the real grid, and the values should not be interpreted as a realistic representation of the Nordic market.

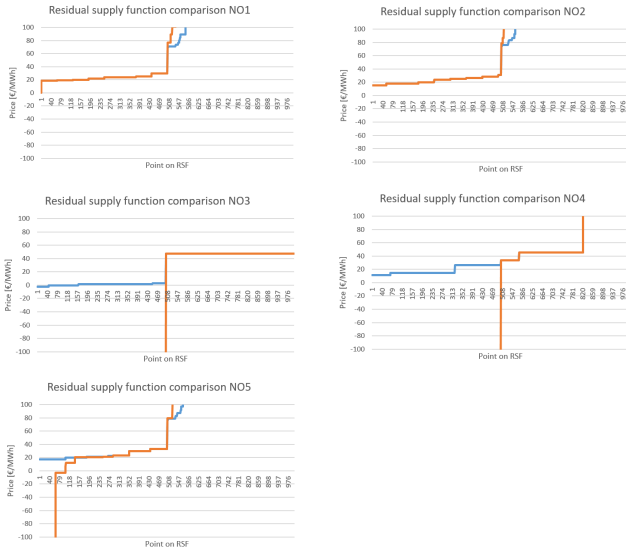


Fig. 3: Comparison of RSFs for tight (in blue) versus loose (in orange) coordination in step 2.

### D. Pricing within Norway

The quantity disaggregation of step 4a (see appendix section D) results in BSP injections, and therefore also flows on the Norwegian network. When we are considering how to price balancing energy, therefore, we can consider BSP activations and flows as fixed parameters. The guiding principle for setting prices is to make prices consistent with what agents are being asked to do by the market clearing model. Failure to do so results in a number of adverse side effects, such as (i) gaming opportunities, (ii) misrepresentation of true costs, or (iii) a tendency for agents to “take matters in their own hands” by removing their resources from the market, e.g. by self-dispatch / self-balancing. This motivates the pricing sub-problem of the disaggregation step which is presented in the appendix. This model aims at setting prices such that the implied value of BSP orders and network utilization is maximized, while minimizing deviations from MARI prices.

### B. Performance Metrics

We record the following performance metrics in our analysis.

**Norway cost:** For solutions that are feasible, what is the implied BSP activation cost for the Norwegian system, compared to the optimal (OPF) cost.

**System cost:** For solutions that are feasible, what is the implied BSP activation cost for the entire system, compared to the optimal (OPF) cost.

**Norway infeasibility:** To what extent does the obtained dispatch violate transmission constraints in Norway. The way in which we quantify this metric is by computing a (linearized) power flow for inferring flows given net injections, and measuring the extent to which these flows violate line flow limits.

**System infeasibility:** To what extent does the obtained dispatch violate transmission constraints in the entire system.

**ADS net financial position:** What is the net cash flow in the “ADS” column of Table III.

**Norwegian TSO net financial position:** What is the net financial position of the Norwegian TSO. This is essentially the sum of the columns “TSO Norway” and “ADS” of Table III. Although from a practical standpoint the desire of a TSO might be for this metric to be close to zero, this is not

guaranteed even in a fully coherent market clearing solution (i.e. a nodal pricing solution).

We further quantify lost opportunity costs of Norwegian BSPs, as well as the lost opportunity cost of the Norwegian TSO [4] in our work. Nevertheless, we do not report these values in the present paper due to space limitations.

### C. Average Results over Multiple Imbalance Realizations

Having discussed the results in a single imbalance realization in section II-B, we now proceed to simulate average performance over 11 imbalance realizations. We use the assumption in [2], equation 3.44, in order to justify the following model of imbalances (we use the same assumptions for the sample drawn in section II-B): we sample a normal random variable with a mean of zero and a standard deviation of 5% of the load of the bus in question. In Table V we present average results for the considered designs.

A loose aggregation results in steep, often price-inelastic, RSFs. Such RSFs can result in extreme levels of MARI prices, which expose the Norwegian TSO to significant settlement imbalances.

The choice between a clairvoyant or non-clairvoyant approach presents tradeoffs. A clairvoyant approach better protects the system at large and the Norwegian network in particular against infeasible MARI clearing positions, and also results in lower cost for both the Norwegian system as well as the entire system. On the other hand, the clairvoyant RSFs typically tend to be steeper (recall that we adopt an optimistic assumption of perfect imbalance forecasts in the clairvoyant model). This exposes the Norwegian TSO to more volatile MARI prices and therefore non-negligible financial imbalances.

The choice between maintaining the price disaggregation of step 4b versus the MARI prices also presents tradeoffs. Maintaining the MARI prices for BSP settlement exposes Norwegian BSPs to significantly misaligned financial incentives, which expose the market operator to gaming as well as self-dispatch (i.e. reduced flexibility in the balancing market). On the other hand, the introduction of step 4b introduces a wedge between the MARI settlement and the ADS disaggregation, which is borne by the TSO.

Overly inflexible RSFs (such as the one based on loose coordination or on clairvoyance) may shield Norwegian zones from infeasible MARI clearing quantities, but they also produce extreme values for MARI clearing prices (with sometimes even greater price separations than those reported in Table II). This can expose the TSO to significant financial imbalances. These financial imbalances can come in two varieties: (i) inter-zonal congestion rents resulting from extreme price differences between Norwegian zones and non-Norwegian zones, and (ii) ADS imbalances for those design options which adopt a nodal price for BSP settlement. The latter financial imbalances are typically significant when the approximation error of the RSF is significant, i.e. when the incremental cost expressed in the RSF (and thus driving the MARI price) is inaccurate relative to the marginal BSP that is activated within Norway in the disaggregation step of the ADS.

## V. CONCLUSION

The paper describes an approach for participation in the upcoming European balancing platforms even if a bidding zone is not a copper plate, which is the assumption of the pan-European balancing platforms. The approach considers constraints within zones by building a Residual Supply Function for each bidding zone, which takes into account those constraints in the bid function that is sent to the platform.

It is possible to consider variations with respect to the construction of the RSF that depend on the following assumptions: (i) whether or not we assume that the zone whose RSF we are constructing can benefit from energy-neutral adjustments of neighboring Norwegian BSPs (a “tight” versus “loose” aggregation), (ii) whether or not we assume that the TSO has knowledge of the imbalances that take place in its system before constructing the RSF (a “clairvoyant” versus “non-clairvoyant” aggregation), and (iii) whether or not we price nodally at the disaggregation stage.

We perform a case study on a 46-node approximation of the Nordic system, where our interest in assessing the viability of the approach for the Norwegian system. The best balance between Norwegian network violations and financial impacts seems to be struck by the baseline approach, which relies on tight coordination, non-clairvoyant aggregation, and price disaggregation. The baseline approach achieves an acceptable level of Norwegian network violations while resulting in moderate MARI price differentials between Norway and neighboring zones, as well as a reasonable alignment between MARI prices and the true incremental costs of the Norwegian zones.

The results so far show that the approach of hierarchical balancing works in principle, but there are still many issues to resolve. Hierarchical balancing is currently being optimized and tested on a realistic model of the Norwegian network. The case study described in this paper indicates points of attention, for instance the price deviations that are observed in section II-B. Further research is underway with Statnett, as well as in the context of TSO-DSO coordination pilots in the FEVER EU H2020 project and the ICEBERG ERC project.

## REFERENCES

- [1] ACER. ACER decision on the implementation framework for mFRR platform: Annex I. implementation framework for the European platform for the exchange of balancing energy from frequency restoration reserves with manual activation in accordance with article 20 of commission regulation (EU) 2017/2195 of 23 November 2017 establishing a guideline on electricity balancing, 2020.
- [2] Jonas Bøe. Balancing energy activation with network constraints, Msc thesis, NTNU, 2017.
- [3] Gerard Doorman, Martin Häberg, Amund S. Øverjordet, Leif Warland, Hallstein Mæland, Åsne Tveita, and Halvor Grønnaas. Handling intra-zonal constraints in the upcoming European balancing markets. In *CIGRE*, 2022.
- [4] M. Garcia, H. Nagarajan, and R. Baldick. Generalized convex hull pricing for the AC optimal power flow problem. *IEEE Transactions on Control of Network Systems*, 7(3):15001510, 2020.
- [5] William W. Hogan. Contract networks for electric power transmission. *Journal of Regulatory Economics*, 4:211–242, 1992.
- [6] N-SIDE. Market approaches for TSO-DSO coordination in Norway. Technical report, Statnett, 2021.
- [7] Anthony Papavasiliou, Mette Bjørndal, Gerard Doorman, and Nicolas Stevens. Hierarchical balancing in zonal markets. In *17th International Conference on the European Energy Market*, 2020.

TABLE V: Performance of different design options over an average of 11 imbalance samples.

	NO cost (€)	System cost (€)	NO infeasibility (MW)	System infeasibility (MW)	ADS net financial position (€)	TSO-NO net financial position (€)
OPF	1421	13657	0	0	N/A	8600
Baseline	4867	13747	6	235	-890	-4456
Loose	4899	13778	6	235	2	21949
Clairvoyant	2930	12659	0	231	-66393	-18282
Loose & clairvoyant	4165	14130	0	229	-264810	-74409

- [8] Hung po Chao and Stephen Peck. Reliability management in competitive electricity markets. *Journal of Regulatory Economics*, 14(2):189–200, 1998.
- [9] Luigi Vanfretti, Svein H. Olsen, Narasimham Arava, Giuseppe Laera, Ali Bidadfar, Tin Rabuzin, Sigurd H. Jakobsen, Jan Lavenius, Maxime Baudette, and Francisco J. Gómez-López. An open data repository and a data processing software toolset of an equivalent Nordic grid model matched to historical electricity market data. *Data in brief*, 11:349–357, 2017.

## APPENDIX

### A. Notation

In this section we present the notation that is used in the models of the paper.

#### Sets

$N$ : set of buses

$G_P/G_B/G_{B,NO}$ : set of plants / balancing plants / Norwegian balancing plants

$L$ : set of loads

$Z$ : set of zones

$K_L/K_T/K_{DC}$ : set of lines / transformers / HVDC lines

$LS$ : set of line groups

$LS_i \subseteq K_T \cup K_L$ : set of lines in line group  $i$

$K_{NO}$ : set of network elements (lines or transformers) which have at least one of their endpoints in the Norwegian zone

$LS_{NO} \subseteq LS$ : subset of line groups with line group members in the Norwegian network

$KL$ : set of MARI links

#### Primal variables

$p_g$ : activated balancing production of plant  $g \in G_B$

$f_k$ : flow of network element  $k \in K = K_T \cup K_L$

$\theta_n$ : voltage phasor angle of bus  $n \in N$

$r_n$ : net injection in bus  $n \in N$

$s_n^+, s_n^-$ : slack variables for constructing residual supply function in step 2

$ls_l$ : load shedding of bus  $l \in L$

$p_{zn}$ : production from residual supply function segment  $n \in \{1, \dots, N_{RSF}\}$  in zone  $z \in Z_{NO}$

$e_z$ : export of zone  $z \in Z_{NO}$  in the price disaggregation model

#### Dual variables

$\rho_n$ : dual variable of power balance constraint of quantity disaggregation model for node  $n \in N$

$\mu_g^+, \mu_g^-$ : dual variable of upper / lower BSP output constraint of BSP  $g \in G_{B,NO}$

$\lambda_k^+, \lambda_k^-$ : dual variable of upper / lower bound on flow limit of line  $k \in K_{NO}$

$\gamma_i^+, \gamma_i^-$ : dual variable of upper / lower limit of line constraint  $i \in LS_{NO}$

$\phi_z$ : dual variable of target export constraint

$\psi_k$ : dual variable of flow definition constraint  $k \in K_{NO} - K_{DC}$

### Parameters

$N_g \in N$ : bus where resource  $g$  is located, where  $g \in G_P \cup G_B \cup L$

$D_l$ : demand of load  $l \in L$

$P_g$ : production of resource  $g \in G_P$

$P_g^+/P_g^-$ : max / min production capacity of resource  $g \in G_B$

$F_k^{Base}$ : baseline flow of power for each Norwegian network element  $k \in K_{NO}$

$FB_k/TB_k \in N$ : from / to bus of network element  $k \in K_T \cup K_L$

$B_k$ : susceptance of network element  $k \in K_T \cup K_L - K_{DC}$

$FM_{axk}$ : line capacity of network element  $k \in K_T \cup K_L$

$LS_i^-, LS_i^+$ : upper and lower line set limit of line-set constraint  $i \in LS$

$A_{ki}$ : coefficient of participation of line  $k \in K_T \cup K_L$  in line-group  $i \in LS$

$MC_g$ : marginal cost of resource  $g \in G_B$

$PTDF_{kn}$ : power transfer distribution factor from bus  $n \in N$  to network element  $k \in K_T \cup K_L - K_{DC}$

$P_g^0$ : fixed production of balancing resource  $g \in G_B$  that is the default state of the unit measured in step 1

$P_g^M$ : change in production of balancing resource  $g \in G_B$  in the MARI platform (i.e. computed in step 3)

$VOLL$ : value of lost load

$V^+$ : penalty parameter for slack variables,  $V^+ > VOLL$

$Imb_z$ : imbalance of zone  $z \in Z$

$FZ_k, TZ_k$ : from / to zone of MARI link  $k \in KL$

$ATC_k^+, ATC_k^-$ : upward / downward ATC capacity of MARI link  $k \in KL$

$N_{RSF}$ : number of breakpoints in residual supply function

$MC_{zn}$ : marginal cost of segment  $n \in \{1, \dots, N_{RSF}\}$  of the residual supply function in zone  $z \in Z_{NO}$

$P_{zn}^+, P_{zn}^-$ : max / min production capacity of segment  $n \in \{1, \dots, N_{RSF}\}$  of the RSF in zone  $z \in Z_{NO}$

$E_z$ : net position of zone  $z \in Z_{NO}$  determined by MARI (steps 2, 3)

$\Pi_z$ : price of Norwegian zone  $z \in Z_{NO}$  determined by MARI (step 3) and used as input for the price disaggregation of step 4b

$P_g^Q$ : BSP position of Norwegian generator  $g \in G_B$ :  $Z_g \in Z_{NO}$  in step 4, which is used as input for step 4b

$W_n$ : weight of Norwegian bus  $n \in N_{NO}$  in the price disaggregation of step 4b

### B. Step 2: Compute Residual Supply Function

In step 2, we aim at computing the residual supply function  $TC_z(E_z)$  of a given zone  $z$  for varying levels of export,  $E_z$ .

The model of step 2 can be described as follows:

$$TC_z(e) = \min_{l_s \geq 0, s \geq 0, p, f, r} \sum_{g \in G_B: Z_g \in Z_{NO}} MC_g \cdot p_g +$$

$$VOLL \cdot \sum_{l \in L: Z_l \in Z_{NO}} l s_l + V^+ \cdot \sum_{n \in N: Z_n} (s_n^+ + s_n^-) \quad (4)$$

$$P_g^- \leq p_g + P_g^0 \leq P_g^+, g \in G_B: Z_g \in Z_{NO} \quad (5)$$

$$l s_l \leq D_l, l \in L: Z_l \in Z_{NO} \quad (6)$$

$$-FMax_k \leq f_k \leq FMax_k, k \in K_{NO} \quad (7)$$

$$f_k = F_k^{Base} + \sum_{n \in N_{NO}} PTDF_{kn} \cdot r_n, \quad (8)$$

$$k \in K_{NO} - K_{DC} \quad (8)$$

$$r_n = \sum_{g \in G_B: N_g = n} p_g + \sum_{l \in L: N_l = n} l s_l + s_n^+ - s_n^-$$

$$- \sum_{k \in K_{DC}: FB_k = n} f_k + \sum_{k \in K_{DC}: TB_k = n} f_k, n \in N_{NO} \quad (9)$$

$$\sum_{n \in N: Z_n = \zeta} r_n = 0, \zeta \in Z_{NO} - \{z\} \quad (10)$$

$$(\pi): \sum_{n \in N: Z_n = z} r_n = E_z \quad (11)$$

$$LS_i^- \leq \sum_{k \in K} A_{ki} \cdot f_k \leq LS_i^+ \quad (12)$$

### C. Step 3: MARI Execution

The model of step 3 can be described as follows:

$$\min_{p, f} \sum_{g \in G_B: Z_g \notin Z_{NO}} MC_g \cdot p_g +$$

$$\sum_{z \in Z_{NO}} \sum_{n=1}^{N_{RSF}} 0.5 \cdot (MC_{zn} + MC_{z, n+1}) \cdot p_{zn} \quad (13)$$

$$ATC_k^- \leq f_k \leq ATC_k^+, k \in K \quad (14)$$

$$\sum_{g \in G_B: Z_g = z} p_g = -Imb_z + \sum_{k \in KL: FZ_k = z} f_k$$

$$- \sum_{k \in KL: TZ_k = z} f_k, z \in Z - Z_{NO} \quad (15)$$

$$\sum_{n=1}^{N_{RSF}} p_{zn} = -Imb_z + \sum_{k \in KL: FZ_k = z} f_k$$

$$- \sum_{k \in KL: TZ_k = z} f_k, z \in Z_{NO} \quad (16)$$

$$P_g^- \leq p_g + P_g^0 \leq P_g^+, g \in G_B: Z_g \notin Z_{NO} \quad (17)$$

$$P_{zn}^- \leq p_{zn} \leq P_{zn}^+, n \in \{1, \dots, N_{RSF}\}, z \in Z_{NO} \quad (18)$$

### D. Step 4a: Quantity Disaggregation

The model of step 4a can be described as follows:

$$(Dis - Q): \min_{p, f, r} \sum_{g \in G_B: Z_g \in Z_{NO}} MC_g \cdot p_g \quad (19)$$

$$P_g^- \leq p_g + P_g^0 \leq P_g^+, g \in G_B: Z_g \in Z_{NO} \quad (20)$$

$$p_g = P_g^M, g \in G_B: Z_g \in Z - Z_{NO} \quad (21)$$

$$\sum_{n: Z_n = z} (r_n - Imb_n) = E_z, z \in Z_{NO} \quad (22)$$

$$r_n = \sum_{g \in G_B: N_g = n} p_g + Imb_n, n \in N \quad (23)$$

$$f_k = F_k^{Base} + \sum_{n \in N} PTDF_{kn} \cdot r_n,$$

$$k \in K_{NO} - K_{DC} \quad (24)$$

$$-FMax_k \leq f_k \leq FMax_k, k \in K_{NO} \quad (25)$$

$$LS_i^- \leq \sum_{k \in K} A_{ki} \cdot f_k \leq LS_i^+, i \in LS_{NO} \quad (26)$$

Note that the net injection variable  $r_n$  is interpreted in this model as the sum of BSP activations *and* imbalances at a given node  $n$ , whereas in the aggregation model of step 2 it is interpreted as only the sum of BSP activations at a given node  $n$ .

### E. Step 4b: Price Disaggregation

The model of step 4b is a linear program that can be described as follows:

$$(Dis - P):$$

$$\min_{\rho, \mu \geq 0, \lambda \geq 0, \gamma \geq 0, \phi, \psi} \sum_{n \in N_{NO}} W_n \cdot (\rho_n - \Pi_{Z_n})^2 \quad (27)$$

$$MC_g - \rho_{N_g} + \mu_g^+ - \mu_g^- \geq 0, g \in G_{B, NO} \quad (28)$$

$$p_g^* \cdot (MC_g - \rho_{N_g} + \mu_g^+ - \mu_g^-) = 0, g \in G_{B, NO} \quad (29)$$

$$\mu_g^- \cdot (p_g^* + P_g^0 - P_g^-) = 0, g \in G_{B, NO} \quad (30)$$

$$\mu_g^+ \cdot (P_g^+ - p_g^* - P_g^0) = 0, g \in G_{B, NO} \quad (31)$$

$$\rho_n + \phi_{Z_n} - \sum_{k \in K_{NO} - K_{DC}} PTDF_{kn} \cdot \psi_k = 0,$$

$$n \in N_{NO} \quad (32)$$

$$\psi_k + \lambda_k^+ - \lambda_k^- + \sum_{i \in LS_{NO}} A_{ki} \cdot \gamma_i^+$$

$$- \sum_{i \in LS_{NO}} A_{ki} \cdot \gamma_i^- = 0, k \in K_{NO} \quad (33)$$

$$\lambda_k^- \cdot (f_k^* + FMax_k) = 0, k \in K_{NO} \quad (34)$$

$$\lambda_k^+ \cdot (FMax_k - f_k^*) = 0, k \in K_{NO} \quad (35)$$

$$\gamma_i^- \cdot \left( \sum_{k \in K_{NO}} A_{ki} \cdot f_k^* - LS_i \right) = 0, i \in LS_{NO} \quad (36)$$

$$\gamma_i^+ \cdot \left( LS_i^+ - \sum_{k \in K_{NO}} A_{ki} \cdot f_k^* \right) = 0, i \in LS_{NO} \quad (37)$$

The starred primal variables correspond to optimal solutions of the quantity disaggregation model of step 4a.